GRZEGORZ W. BĄK

Institute of Physics, Lodz University of Technology, ul. Wólczańska 219, 90-924 Łódź, Poland, e-mail: grzegorz.bak@p.lodz.pl

DISPERSIVE CHARGE TRANSPORT IN HOPPING SYSTEMS UNDER OPEN-CIRCUIT CONDITIONS: COMPUTER SIMULATION

Applicability of the theories describing the discharge in thin-film insulators under open-circuit conditions for dispersive hopping systems is the subject of this paper. It is shown by means of computer simulation that the drift mobility obtained from application of the theories for such systems is underestimated. The computer simulation was carried out for a thin film system in which the charge transport is dominated by hopping of charge carriers among localized states in a narrow band at the Fermi level. The way of interpretation of the discharge under open-circuit conditions in such systems is suggested. The simulation results have also been applied for interpretation of the open-circuit discharge in thin diamond-like carbon films.

Keywords: low-mobility materials, dispersive transport.

1. INTRODUCTION

The main experimental method used for measurements of mobility of charge carriers in low-mobility disordered materials is the so-called time-of-flight (TOF) method [1, 2]. The method consists in measuring the transient currents which is caused by charge carriers injected into a sample at a surface and moving in the external electric field. The drift mobility μ may be calculated from the equation:

$$\mu = \frac{D^2}{V_0 t_{tr}} \tag{1}$$

where D is the sample thickness, V_0 is the voltage applied, t_{tr} is the transition time of charge through the sample. The transition time corresponds to a "kink"

on the current pulse. The spatial concentration of moving charge packet remains Gaussian during the transport. This kind of charge transport is often called a Gaussian type of transport.

A number of experimental data obtained for amorphous and strongly doped materials cannot be interpreted in this simple way because no "kink" on the current pulses is detected. Such non-classical data can be understood in terms of the model of stochastic hopping presented by Scher and Montroll [3] in 1975. The current pulses in Scher-Montroll (SM) model is given by:

$$i(t) \propto t^{-(1-\alpha)} \qquad \text{for } t < t_{tr} \qquad (2)$$

$$i(t) \propto t^{-(1+\alpha)} \qquad \text{for } t > t_{tr} \qquad (3)$$

where the disorder parameter α is constant. The transition time found from equations (2) and (3) corresponds to the time of transport of the fastest charge carriers. This kind of charge transport is often called a dispersive transport. It was shown during the next few years that both multiple trapping [4-7] and trap-controlled hopping [8] may also give rise to the dispersive transport of charge. It has also been shown by means of computer simulation [9] that for some temperatures the hopping transport in a narrow band of localized states can also lead to the dispersive transport if the width of the band is big enough.

In case of very thin samples we often have to do with a short circuit originating during evaporation of electrodes. In this case the classical TOF method cannot be used for estimation of the drift mobility of charge carriers. However, the discharge under open circuit conditions may be a suitable method to find the drift mobility in such systems. The theory describing the discharge under open circuit conditions in thin film insulators was given by Batra et.al. [10]. The metalized surface is grounded, the free surface is charged using either a corona discharge [11, 12] or a low-energetic electron beam [13-15]. The time dependence of the voltage between the two surfaces is given by [10]:

$$V(t) = V_0 - \frac{\mu V_0^2}{2D^2} t \qquad (4)$$

$$\frac{dV}{dt} = -\frac{\mu V_0^2}{2D^2} \qquad (5)$$

for $t < t_{tr}$ and

$$V(t) = \frac{D^2}{2\mu} \frac{1}{t} \qquad (6)$$

$$\frac{dV}{dt} = -\frac{D^2}{2\mu}\frac{1}{t^2} \tag{7}$$

for $t > t_{tr}$. It results from Batra model and equations (4)÷(7) that the time corresponding to $V = 0.5\ V_0$ (V_0 is the voltage at the time $t = 0$) is the transit time of charge carriers.

The problem of applicability of equations (4)÷(7) for open-circuit discharge in hopping systems in these cases, in which a "kink" on the current pulses obtained from the classical TOF experiments is observed, have been discussed previously [9]. The aim of this paper is to discuss the problem of applicability of equations (4)÷(7) for the so-called dispersive hopping systems. The simulation results were also used for reinterpretation of the open-circuit discharge in thin diamond-like carbon films.

2. ASSUMPTIONS OF THE SIMULATION

The basic physical assumptions of simulation were as follows [16]:
1. The charge transport is dominated with hopping in a narrow band of localized states at the Fermi level.
2. The probability of a jump between i and j state was taken in the form[17]:

$$p_{ij} = \nu_{ph}\exp(-2\alpha R_{ij})\exp(\frac{-(E_j - E_i - eF(x_j - x_i))}{kT}) \tag{8a}$$

for $E_j-E_i-eF(x_j-x_i)>0$

$$p_{ij} = \nu_{ph}\exp(-2\alpha R_{ij}) \tag{8b}$$

for $E_j-E_i-eE(x_j-x_i)<= 0$, where e is the electron charge, E_i, E_j are the energies of i- and j-states, x_i, x_j are the positions of the states measured along the electric field and F is the intensity of electric field.
3. The values of localization parameter $2\alpha R = 3,5,7,9,11,13$ were taken (α is the electron localized wave-function, R is the distance between the localized states).
4. The distribution of the state energies is the normal one and is described by the standard deviation σ_E, which changes in the range 0.01÷0.16 eV.
5. The temperature changes in the range between 100 K and 500 K.

The algorithm of the simulation was described in [9]. The algorithm used was tested for the classical TOF experiment and a good agreement between the results of simulation and the theoretical description of hopping transport was obtained [9].

In order to solve the problem of applicability of equations (4)÷(7) for interpretation of discharge under open-circuit conditions in dispersive hopping systems one has to compare the results of drift mobility resulting from application of equations (4)÷(7) with the real value of drift mobility in these systems. The real value of drift mobility for this comparison can be obtained in two ways:

1. The values can be calculated from the theoretical formulae describing the hopping transport in a narrow band of localized states [18]:

$$\mu = \frac{eR^2}{6kT} v_{ph} \exp(-2\alpha R) \exp\left(\frac{-W}{kT}\right) \qquad (9)$$

   where R is the distance between the states, k is the Boltzmann constant, T is the temperature, v_{ph} is the phonon frequency, W is the effective activation energy related to the width of the band of localised states. However, the above expression is very sensitive to the assumed value of W. Though the approximate relation between the effective activation energy W and the standard deviation σ_E was given previously [9], it is obvious that the comparison with the mobility estimated from equation (8) would be burdened with some systematic error resulting from the inaccuracy of determination of W. For instance assuming $W = 2\sigma_E$ or $W = 4\sigma_E$ we obtain the ratio of the resulting mobilities $\mu(2\sigma_E)/\mu(4\sigma_E)$ (at T = 300 K) close to 1 order of magni-tude for $\sigma_E = 0.03$ eV and exceeding 2 orders of magnitude for $\sigma_E = 0.07$ eV.

2. The real values of drift mobility can be obtained from simulation of charge transport in the classical TOF experiment. In case of dispersive transport (which is a subject of this paper) the current pulses obtained from the simulation (when no "kink" on the current curves is detected) should be interpreted using SM model (equations (2) and (3)). The mobility obtained in this way is to be compared with the mobility obtained from Batra theory describing the discharge under open-circuit conditions (i.e. with $\mu_{1/2}$ resulting from equations (4)÷(7) for t_{tr} corresponding to the voltage $V = 0.5 V_0$). This second way of comparison enables to avoid any systematic errors resulting from application of equation (8), because the only difference between the two simulations is the kind of simulated experiment (the discharge under open circuit conditions is the subject of the first simulation, the transport in the classical TOF experiment in order to obtain the real value of mobility for comparison is a subject of the second simulation).

3. In this situation the mobility obtained from simulation of charge transport in the classical TOF experiment was taken for our comparison.

3. RESULTS

3.1. Simulation results

The obtained values of $\mu_{real}/\mu_{1/2}$ are shown in Tables 1÷5. The tables summarise both the results obtained for Gaussian transport published earlier ([9], *italic*) and the results concerning the dispersive transport (**bold**) which in general occur for the higher values of the standard deviation σ_E defining the width of band of localised states (for details see [9]). In order to interpret the data properly one should estimate the error of the points obtained from the simulation. The error consists of two components. The first one results from the technical treatment of the voltage-time pulses obtained from the simulation. In order to find the $\mu_{real}/\mu_{1/2}$ ratio one must find the time of flight both for the classical TOF experiment and for the open-circuit discharge. Both the times are burdened with some error. The second component of the error results from the stochastic nature of the process simulated which means, that for a number of simulations carried out for the same starting parameters the value of the time of flight can differ a little. The total error of the obtained $\mu_{real}/\mu_{1/2}$ ratios was esti-mated as 20%. Fig. 1 shows the simulation data for the two temperatures 200 K and 500 K at $\sigma_E = 0.05$ eV.
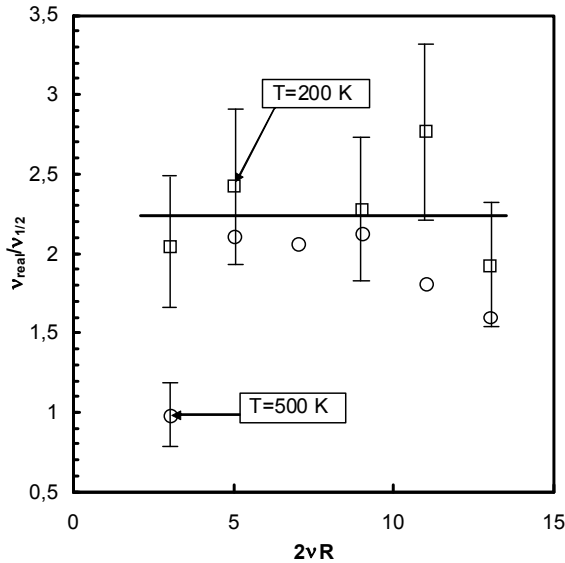

Fig. 1. $\mu_{real}/\mu_{1/2}$ as a function of the localisation parameter $2\alpha R$ for T = 200 K (□) and T = 500 K (o). $\sigma_E = 0.05$ eV. The full line corresponds to the $\mu_{real}/\mu_{1/2}$ ratio estimated for T = 200 K.

Table 1. The ratio $\mu_{real}/\mu_{1/2}$ for various values of the localization parameter $2\alpha R$ and the standard deviation σ_E at T = 100 K. *Italic=Gaussian transport,* **bold=dispersive transport.**

σ_E [eV] $2\alpha R$	0.01	0.02	0.03	0.04	0.05	0.06	0.07	0.08
3	*1.58*	*1.64*	*2.03*	*2.11*	**2.28**	**2.33**	**2.42**	**2.58**
5	*1.81*	*2.35*	*2.77*	*3.82*	*4.74*	--	--	--
7	*2.19*	*3.18*	*3.94*	*3.62*	*5.01*	--	--	--
9	*2.02*	*2.78*	**3.02**	**3.57**	**3.82**	--	--	--
11	*1.80*	--	--	--	--	--	--	--
13	*1.38*	--	--	--	--	--	--	--

Table 2. The ratio $\mu_{real}/\mu_{1/2}$ for various values of the localization parameter $2\alpha R$ and the standard deviation σ_E at T = 200 K. *Italic=Gaussian transport,* **bold=dispersive transport.** The values for σ_E equal to 0.01 eV and 0.02 eV are not shown and can be found in [9].

σ_E [eV] $2\alpha R$	0.03	0.04	0.05	0.06	0.07	0.08	0.09	0.10	0.11	0.12
3	*1.73*	*1.57*	*2.05*	**2.81**	**2.88**	**2.76**	**2.72**	**3.06**	**3.05**	**3.54**
5	*1.50*	*2.59*	*2.43*	*2.17*	**2.22**	**2.22**	**2.75**	*2.72*	*2.84*	*3.37*
7	*2.18*	*2.36*	--	**2.09**	**2.22**	**2.44**	**2.33**	--	--	--
9	*2.22*	**2.12**	**2.28**	**2.33**	**2.64**	**2.79**	**2.81**	--	--	--
11	*2.31*	*2.41*	*2.77*	--	--	--	--	--	--	--
13	*1.84*	*2.02*	*1.93*	*3.02*	--	--	--	--	--	--

Table 3. The ratio $\mu_{real}/\mu_{1/2}$ for various values of the localization parameter $2\alpha R$ and the standard deviation σ_E at T = 300 K. *Italic=Gaussian transport,* **bold=dispersive transport.** The values for σ_E equal to 0.01 eV and 0.02 eV are not shown and can be found in [9].

σ_E [eV] $2\alpha R$	0.03	0.04	0.05	0.06	0.07	0.08	0.09	0.10	0.11	0.12
3	*1.58*	*1.41*	*1.62*	*1.85*	*1.83*	**2.36**	**2.25**	**2.03**	**2.26**	**2.32**
5	*2.50*	*2.17*	*2.65*	*2.38*	**2.79**	**2.21**	**2.55**	**1.62**	**1.94**	**2.52**
7	*2.31*	*2.57*	*1.88*	**2.52**	**2.39**	**2.40**	**1.88**	**1.78**	**2.16**	**2.07**
9	*2.22*	--	--	**2.34**	**2.20**	**1.94**	**1.80**	**2.63**	**2.59**	**3.49**
11	*1.78*	*1.96*	*2.15*	*2.2*	*1.89*	--	--	--	--	--
13	*1.66*	*2.11*	*1.97*	*2.06*	*2.19*	*2.12*	--	--	--	--

Table 4a. The ratio $\mu_{real}/\mu_{1/2}$ for various values of the localization parameter $2\alpha R$ and the standard deviation σ_E at T = 400 K. *Italic=Gaussian transport,* **bold=dispersive transport.** The values σ_E between 0.01 eV and 0.07 eV are presented.

σ_E [eV] $2\alpha R$	0.01	0.02	0.03	0.04	0.05	0.06	0.07
3	*1.34*	*1.30*	*1.46*	*1.41*	*1.49*	*1.50*	*1.53*
5	*1.99*	*1.65*	*1.88*	*2.11*	*2.22*	*2.64*	**2.41**
7	*2.83*	*2.80*	*2.90*	*2.50*	*3.16*	**2.02**	**1.88**
9	*1.93*	*2.16*	*1.90*	*2.16*	*2.13*	**1.77**	**1.45**
11	*1.68*	*1.84*	*1.76*	*1.69*	*1.83*	*1.78*	*1.71*
13	*1.54*	*1.72*	*1.70*	*1.96*	*1.78*	*1.97*	*1.94*

Table 4b: The ratio $\mu_{real}/\mu_{1/2}$ for various values of the localization parameter $2\alpha R$ and the standard deviation σ_E at T = 400 K. *Italic=Gaussian transport,* **bold=dispersive transport.** The values σ_E between 0.07 eV and 0.14 eV are presented.

σ_E [eV] $2\alpha R$	0.08	0.09	0.10	0.11	0.12	0.13	0.14
3	**1.98**	**2.22**	**2.10**	**2.00**	**2.25**	**1.92**	**1.84**
5	**2.27**	**1.71**	**1.89**	**2.34**	**1.74**	--	--
7	**2.04**	**2.01**	**1.82**	**1.69**	**2.01**	--	--
9	**2.10**	**2.03**	**2.23**	**1.98**	**2.80**	--	--
11	--	--	--	--	--	--	--
13	*1.89*	--	--	--	--	--	--

Table 5a. The ratio $\mu_{real}/\mu_{1/2}$ for various values of the localization parameter $2\alpha R$ and the standard deviation σ_E at T = 500 K. *Italic=Gaussian transport,* **bold=dispersive transport.** The values σ_E between 0.01 eV and 0.08 eV are presented.

σ_E [eV] $2\alpha R$	0.01	0.02	0.03	0.04	0.05	0.06	0.07	0.08
3	*1.08*	*1.01*	*1.08*	*0.96*	*0.98*	*1.04*	*1.04*	**1.48**
5	*2.02*	*2.14*	*2.06*	*1.78*	*2.11*	*2.44*	**2.06**	**2.31**
7	*2.01*	*2.15*	*2.26*	*2.59*	*2.06*	**2.04**	**1.83**	**1.69**
9	*1.93*	*2.17*	*1.90*	*2.16*	*2.13*	**1.58**	**1.69**	**1.84**
11	*1.69*	*1.82*	*1.80*	*1.70*	*1.81*	*1.89*	*1.71*	--
13	*1.55*	*1.62*	*1.65*	*1.91*	*1.60*	*2.02*	*1.83*	--

Table 5b. The ratio $\mu_{real}/\mu_{1/2}$ for various values of the localization parameter $2\alpha R$ and the standard deviation σ_E at $T = 500$ K. *Italic=Gaussian transport,* **bold=dispersive transport.** The values σ_E between 0.09 eV and 0.16 eV are presented.

σ_E [eV] $2\alpha R$	0.09	0.10	0.11	0.12	0.13	0.14	0.15
3	**1.40**	**1.50**	**1.53**	**1.70**	**1.61**	**1.42**	**1.69**
5	**2.18**	**1.61**	**1.91**	**1.57**	**1.57**	**1.61**	**1.78**
7	**1.82**	**1.93**	**1.87**	**2.04**	**2.05**	**1.93**	--
9	**1.74**	**1.89**	**2.34**	**2.08**	**2.01**	**2.35**	--
11	--	--	--	--	--	--	--
13	--	--	--	--	--	--	--

The errors for the data corresponding to 200 K are also depicted in this figure. It results from the figure that for all the values of $2\alpha R$ the $\mu_{real}/\mu_{1/2}$ ratio may be assumed to exceed 2 a little for $T = 200$ K. The data for 500 K shows the ratio to be a little lower. One point obtained for the lowest value of $2\alpha R$ (corresponding to the Gaussian transport) diverges significantly from the others. This means that for the lowest values of αR (i.e. for the weaker localisation of the localised electron wave-function) the ratio $\mu_{real}/\mu_{1/2}$ drops down from its most frequent value of about 2. This is confirmed by Fig. 2 showing the function $\mu_{real}/\mu_{1/2}$ vs. the standard deviation σ_E for $T = 500$ K and $2\alpha R = 3$. For all the cases of the
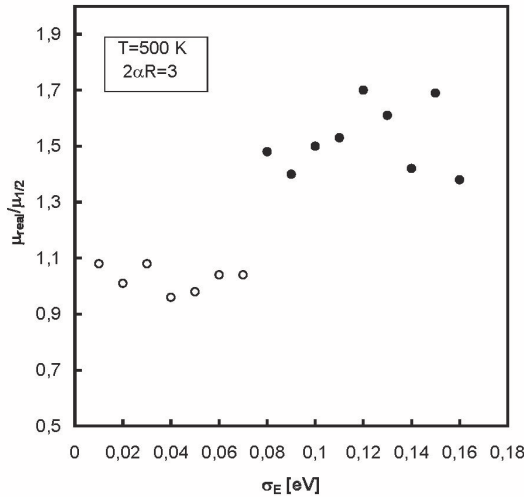

Fig. 2. $\mu_{real}/\mu_{1/2}$ as a function of the standard deviation σ_E describing the energetic disorder of the system. o − Gaussian transport, • − dispersive transport. $T = 500$ K, $2\alpha R = 3$.

Gaussian transport (occurring up to $\sigma_E = 0.08$ eV) the ratio $\mu_{real}/\mu_{1/2}$ remains close to 1, starting to increase at $\sigma_E = 0.08$ eV, for which the dispersive transport begins to dominate. It seems that the increase of the ratio $\mu_{real}/\mu_{1/2}$ for the dispersive transport takes place for the lowest value of αR first of all (see also Tables 1÷5) except for the temperature 100 K, where the increase is not so evident. For the higher values of αR the change of the kind of transport does not influence the value of $\mu_{real}/\mu_{1/2}$ so evidently. For instance, the ratio can be regarded equal to about 2 for all values of σ_E at $2\alpha R = 9$ (see Fig. 3). It results from the data
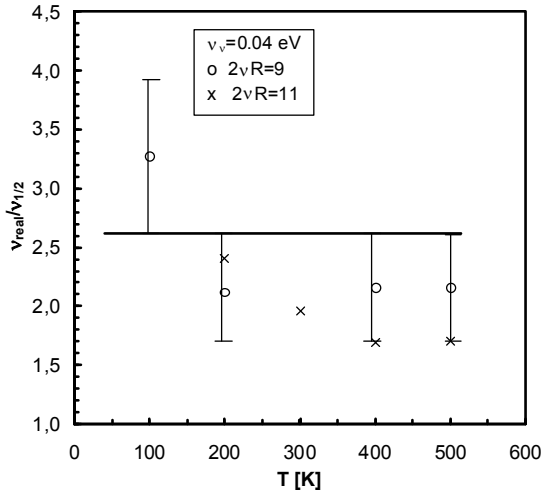

Fig. 3. $\mu_{real}/\mu_{1/2}$ as a function of the standard deviation σ_E describing the energetic disorder of the system. o – Gaussian transport, • – dispersive transport. T = 500 K, $2\alpha R = 9$.

presented in the tables that the values of drift mobility in dispersive hopping systems obtained from direct application of Batra model are underestimated. The ratio $\mu_{real}/\mu_{1/2}$ is close to 2 for the most of the cases investigated. No clear difference (except for the lower values of αR) in this ratio for Gaussian transport and the dispersive transport has been found. Having the data depicted in Tables 1÷5 and the estimated values of σ_E and $2\alpha R$ one can estimate the real value of drift mobility in a hopping system from the discharge pulses obtained under open-circuit conditions. An example of application of the simulation results for experimental data is presented in section 3.2.

2.2. Comparison with experimental results

Diamond-like carbon (DLC) thin films is an example of an amorphous system, in which the charge transport is dominated with hopping transport in a narrow band of localised states [13-15]. The values of the drift mobility $\mu_{1/2}$ found from the discharge curve are shown in Fig. 4 [13]. The values of the parameter α^{-1} in DLC films was found to be about 1.0÷1.2 nm [19].
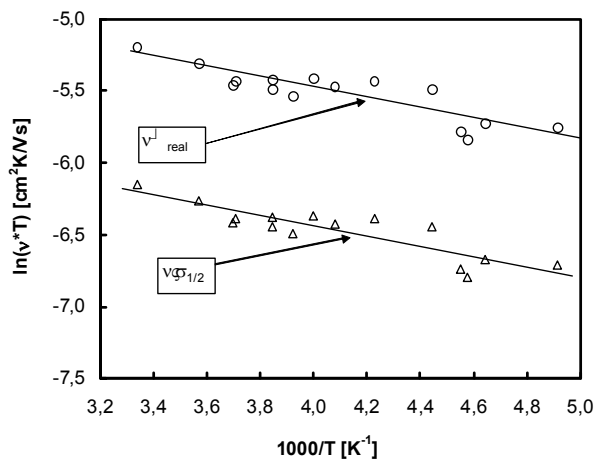

Fig. 4. Drift mobility of electrons in DLC thin films. Δ − mobility values obtained directly from Batra model [13], • − real values of mobility obtained from the factor $\mu_{real}/\mu_{1/2}$ resulting from Fig. 3.
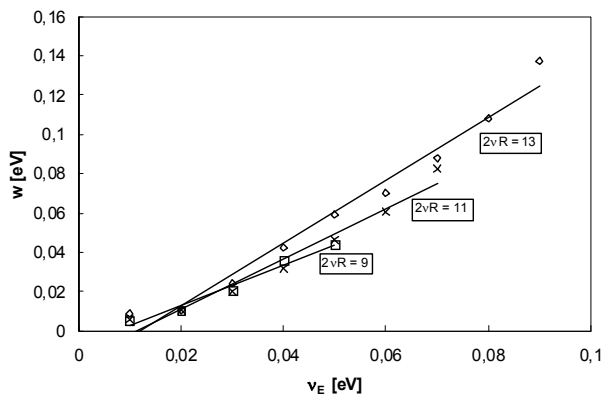

Fig.5. Relations between the activation energy of mobility and the standard deviation σ_E for various values of $2\alpha R$. The relations are described by the equations: for $2\alpha R = 9$ W = $1.0366\sigma_E$-0.0079 eV; for $2\alpha R = 11$ W = $1.2716\sigma_E$-0.0141 eV; for $2\alpha R = 13$ W = $1.6029\sigma_E$-0.0192 eV.

The average distance of R in DLC films was found to be 5÷7 nm [20]. This gives the value of $2\alpha R$ equal to about 10. To find the ratio $\mu_{real}/\mu_{1/2}$ one must find the value of the standard deviation σ_E for the case investigated. This can be found from the data published previously [9] and for completeness and clarity of the paper presented in Fig. 5. As seen from the figure, the value of σ_E corresponding to the experimentally found activation energy $W = 0.03$ eV [13, 20] is close to 0.04 eV. Fig. 6 shows the ratio $\mu_{real}/\mu_{1/2}$ for both $2\alpha R = 9$ and $2\alpha R = 11$ assuming $\sigma_E = 0.04$ eV. The figure shows, that for the case considered the ratio $\mu_{real}/\mu_{1/2}$ is close to 2.6. This enables to find the real values of the mobility presented in Fig. 6 to compare the values to those obtained directly from Batra model.
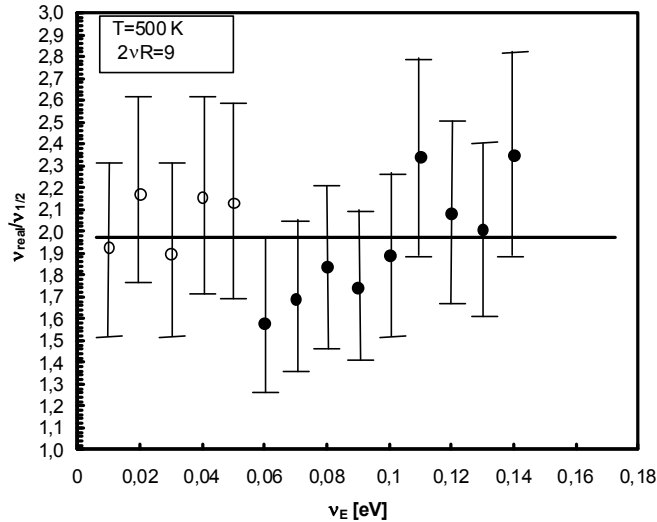

Fig. 6. $\mu_{real}/\mu_{1/2}$ ratio for $\sigma_E = 0.04$ eV and $2\alpha R = 9$ and $2\alpha R = 11$. The full line gives the ratio for the parameters which result from the estimations given in the text.

3. CONCLUSIONS

The following conclusions result from the presented simulation data:
1. In case of systems dominated with hopping transport the drift mobility obtained from direct application of Batra model is usually underestimated both for the case of Gaussian and dispersion transport. Only for the higher temperatures (T = 500 K) and weak localisation ($2\alpha R = 3$) direct application of Batra model gives correct results.

2. For most of the cases investigated the ratio $\mu_{real}/\mu_{1/2}$ is close to 2 regardless of the kind of transport dominating. However, for some cases (weak localisation $2\alpha R = 3$, high temperatures) the change of kind of transport leads to detectable change of the ratio $\mu_{real}/\mu_{1/2}$.

3. In general the ratio $\mu_{real}/\mu_{1/2}$ slightly increases with increasing standard deviation σ_E describing the off-diagonal disorder, though in some cases the increase is not quite evident and could be interpreted as stochastic oscillations within the simulation error.

REFERENCES

 [1] **Spear W.E.,** Proc. Phys. Soc., **B70** (1957) 669.
 [2] **Spear W.E.,** J. Non-Crystalline Solids **1** (1969) 197.
 [3] **Scher H. and Montroll E.W.,** Phys. Rev. **B12** (1975) 2455.
 [4] **Noolandi J.,** Phys. Rev. **B16** (1977) 4466.
 [5] **Noolandi J.**, Phys. Rev. **B16** (1977) 4474.
 [6] **Schmidlin F.W.,** Solid St. Commun. **22**(1977) 451.
 [7] **Schmidlin F.W.,** Phys. Rev. **B16** (1977) 2362.
 [8] **Pfister G., Scher H.,** Adv.Phys. **27** (1978) 747.
 [9] **Stępnik P., Bąk G.W.,** J. Phys.: Condensed Matter **12** (2000) 8455.
[10] **Batra I.P., Kanazawa K.K. and Seki H.,** J. Appl. Phys. **41** (1970) 3416.
[11] **Enck R.C., Abkowitz M.,** J. Non-Crystalline Solids **66** (1984) 255.
[12] **Sonnonstine T.J., Perlman M.M.,** J. Appl. Phys. **46** (1975) 3975.
[13] **Mycielski W., Staryga E., Lipiński A., Dłużniewski M.,** Elektron Technology **27** (1994) 29.
[14] **Mycielski W., Staryga E., Lipiński A.,** Thin Solid Films **235** (1994) 13.
[15] **Mycielski W., Staryga E., Lipiński A., Mitura S., Sokolowska A.,** Diamond and Related Materials **3** (1994) 858 .
[16] Computer programme was developed by P. Stępnik.
[17] **Bassler H.,** Phys. Stat. Sol. **B107** (1981) 9.
[18] **Mott N.F. and Davis E.A.,** "Electronic Processes in Non-Crystalline Materials" (Clarendon, Oxford 1971).
[19] **Robertson J.,** Prog. Solid St. Chem. **21** (1991) 199.
[20] **Mycielski W., Staryga E., Dłużniewski M., Strzelecki W.,** Latvian J. Phys. Tech. Sci. **6** (1994) 3.

DYSPERSYJNY TRANSPORT ŁADUNKU W UKŁADACH PRZESKOKOWYCH W WARUNKACH OBWODU OTWARTEGO: SYMULACJA KOMPUTEROWA

Streszczenie

Badano stosowalność teorii opisujących rozładowanie cienkich warstw izolatorów z przeskokowym transportem ładunku w warunkach obwodu otwartego. Pokazano, że wartości ruchliwości otrzymane w wyniku zastosowania tych teorii do układów dyspersyjnych są niedoszacowane. Symulację wykonano dla układów, w których transport przeskokowy odbywa się w wąskim paśmie w pobliżu poziomu Fermiego. Otrzymane wyniki zastosowano do reinterpretacji wyników badań ruchliwości w warstwach DLC.